Design and Analysis of an Energy-Efficient Hovercraft

Sajed Rezaei, Hüseyin Ayhan Yavaşoğlu*

Mechatronics Department, Yıldız Technical University, Istanbul, Turkey

hayhan@yildiz.edu.tr *Email of the corresponding author*

Abstract – This study discusses the design and analysis of an electric-powered hovercraft with an emphasis on safety and operability. Beginning with a computational fluid dynamics (CFD) analysis, the optimal, energy-efficient shape for the hovercraft is determined based on air drag force and trajectories flow around the hovercraft's body. On the basis of the CFD analysis results, a workable 3D model is developed in Solidworks. Using several formulas to calculate the required motor power and characteristics for both the lift and propulsion motors, the system topology and component selection for a proposed small-scale model are specified. In addition to CFD analyses, mechanical analyses are performed to ensure that the various components of the hovercraft can withstand the forces acting on them, these studies are based on Solidwork's static analyses. Various electronic components, BLDC motors, motor drivers, servo motor, and sensors are connected to the Raspberry Pi (RPi), which serves as the hovercraft's primary controller. This paper provides a comprehensive overview of the design and analysis of the electric-powered hovercraft, including the selection of key components and the results of CFD and mechanical analyses to ensure the safety and operability of the hovercraft. Discussed methods in this article can be used for further studies on the energy efficiency of hovercrafts.

Keywords - Hovercraft, CFD, Mechanical Analysis, Energy Efficiency, 3D Design

I. INTRODUCTION

Hovercrafts are versatile vehicles, capable of moving on almost any surface (for example land, water, mud, ice, and more. This amphibious feature makes them highly suitable for conducting rescue operations and carrying heavy payloads over unconventional surfaces [1].

Forward motion in hovercrafts is created by air propulsion fans, combining these fans with a rudder system provides maneuverability and motion stabilization. Studies have been conducted on motion control and stability of small-scale hovercrafts on different surfaces [2]-[5].

The lift fan is a crucial component of a hovercraft, responsible for generating the lift force that allows the vehicle to hover above the ground or water. Depending on the size and weight of the hovercraft, the size and shape of the lift fan can vary, with larger vehicles requiring more powerful fans to generate the necessary lift force. Typically, hovercraft lift fans operate either manually or at full load capacity, resulting in significant energy inefficiency and waste.

Several studies and books have been published regarding the general principles of hovercrafts. These studies include information about the air-cushion theory, stability of the hovercrafts, and required motor calculations [1], [6]-[8]. However, they are mostly based on old-schooled large hovercrafts with fossil-fueled engines.

The ability of hovercrafts to achieve their maximum operational duration is of the utmost importance, especially when powered by electricity. To reduce the air drag, which increases in proportion to the square of the vehicle speed, it is essential to incorporate flow analysis into the design phase. By employing computational fluid Dynamics

(CFD) simulations, we can visualize and quantify these effects in a computer-simulated environment [9]-[10]. Although CFD simulations have been performed on hovercrafts in prior research [11], these studies have only focused on the external analysis of the hovercraft's body, ignoring internal simulations.

Despite their numerous benefits, hovercrafts suffer from a significant drawback: their high energy consumption, which limits their operational duration and ability to conduct long-distance operations. A limited number of research works exist on the energy efficiency of hovercrafts. One such study examines the energy consumption of an autonomous hovercraft model and discusses practical test outcomes and mechanical design characteristics to reduce hovercraft energy consumption [12]-[13]. However, although this study is commendable, it overlooks the significance of flow simulation and various control techniques for enhancing energy efficiency

Therefore, the focus of this study is on more efficient hovercraft design utilizing various CFD analyses. In addition to the analysis of flow characteristics for multiple vehicle components, the selection of components and system topology for a scale model to be used in upcoming experimental tests is also included.

II. Materials and Method

A. Hovering

A hovercraft can hover because of a flexible cushion that is placed at the bottom of the hovercraft, attached to the main hull. The lift fan blows the air into the plenum chamber (which is placed inside the main hull's body), then air is directed to the cushion. The blown air cushion lifts the hovercraft from the ground. Air escaping from the cushion creates a barrier that reduces friction and allows the hovercraft to move easily.

To choose the required lift motor, the required gauge pressure at the bottom of the air cushion should be calculated. The required information can be obtained using the following equation. [14]

$$P_r = \frac{m \times g}{A} \qquad (1)$$

Where *m* represents the total mass of the hovercraft (including the payload), *g* represents the gravitational acceleration and *A* represents the area of the air cushion. It should be noted that the aforementioned formula only provides a rough estimate and does not account for the various energy losses that can occur during operation. In this study, CFD simulations will be discussed in chapter III to consider the losses and produce a more accurate result.

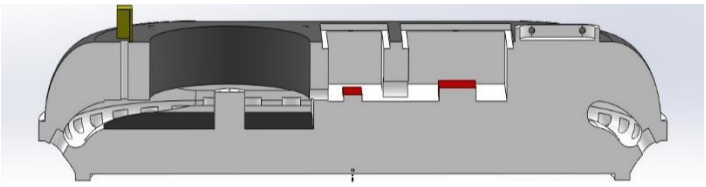

Fig. 1 Cross-sectional view of the proposed model's plenum chamber

B. Propulsion

In the following section, a comprehensive analysis of the distinct forces that impede the forward motion of a hovercraft and that the propulsion motor must overcome will be presented.

- *Climbing Force*

The aforementioned force is associated with hovercraft operations on an inclined plane, and can be computed as follows [14]:

$$F_{cl} = m \times g \times Sin\emptyset \qquad (2)$$

Where F_{cl} is the required climbing force, *m* is the mass of the hovercraft, g is gravitational acceleration, and $\emptyset$ is the slope angle.

- *Aerodynamic Drag Force*

The molecules of air are quite small. Millions of small forces are created when a solid object moves through the air because of interactions with all of these molecules. The aerodynamic drag force is the force of these molecules acting on the solid object as it moves forward. This force should be overcome since it acts like a friction force and slows the movement. It depends on many variables such as the cross-sectional area of the hovercraft, air density, and geometrical parameters, and can be calculated with the following formula [15]:

$$F_D = \frac{1}{2} \times \rho \times A \times C_d \times V^2 \qquad (3)$$

Where F_D is the aerodynamic drag force acting on the hovercraft, ρ is the air density, A is the cross-sectional area of the hovercraft, C_d is the drag coefficient, and V is the speed of the hovercraft.

- *Acceleration Force*

Required acceleration force can be obtained by the following formula, not that this force acts when the hovercraft is accelerating: [14]

$$F_a = m \times a \tag{4}$$

Where F_a is the acceleration force, m is the mass of the hovercraft, and a is the acceleration.

Also, we should consider kinematic formulas to further study the acceleration force:

$$v = v_0 + at \tag{5}$$

Where v is the final velocity of the hovercraft, v_0 is the initial velocity of the hovercraft, and t is the time to reach the required speed.

- *Total Required Thrust Force*

The friction force between surfaces has been neglected in the hovercraft system due to the creation of an air cushion that generates a low-friction surface. By considering the required and acting forces on the hovercrafts, the total required thrust force can be calculated as follows:

$$F_t = F_d + F_{cl} + F_a \tag{6}$$

C. Electronics and Block Diagram

This section provides an overview of the proposed topology of the scaled hovercraft system and the key characteristics of the selected components. This information is provided to facilitate the experimental tests that will be conducted as part of the ongoing study.

As a single-board computer (SBC) for supervisory control of all systems, Raspberry Pi (RPi) is selected. The Raspberry Pi camera is used to provide the hovercraft's front view, allowing the user to remotely control it with a mobile phone. The hovercraft can be controlled with a wireless connection between the mobile phone and the RPi; the user logs into the controller with a username and password to access the camera feed of the hovercraft and control functions.

Two brushless DC motors (BLDC) are utilized for lift and propulsion systems, these motors are controlled with electronic speed controllers (ESC) that are connected to the RPi and can regulate the speed of the BLDC motors.

The rudder system is controlled by a servo motor that is capable of adjusting the angle of the rudders and altering the yaw axis' direction. The angle of the rudder responds to the user's inputs via the app's turn left and turn right functions.

An inertial measurement unit (IMU) sensor provides nessecery information such as orientation, angular velocity, and linear acceleration of the hovercraft which is used for guiding and controlling the hovercraft.

A pressure sensor measures the air pressure in the cushion of the hovercraft, and a load sensor measures the weight of the payload that the hovercraft is carrying. This information will be used to adjust the revolutions per minute (RPM) of the lift fan and optimize its usage.

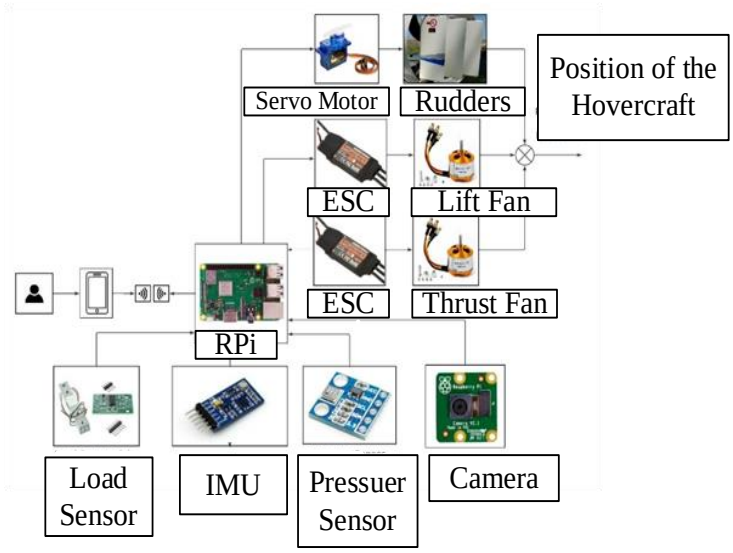

Fig. 2 Block diagram of the system

III. PROPOSED MODEL

A. CFD Analysis to Determine Overall Shape

In the scope of this project, CFD analyses of airflow around the three primary proposed shapes have been conducted to determine which shape has the most energy-efficient characteristics. At the outset of our studies, we examined three rough models with roughly the same dimensions. The

dimensions of the models and evaluation criteria are provided in Table 1.

Table 1. Dimension of the test models

Model Parameter	Value
Max Dimesnsions	50x25x17.5 cm
Velocity of the Model	2 m/s
Pressure	101325 Pa
Temperature	293.2 K

Figure 3 depicts the results of the airflow simulations performed with the Solidworks software. The results indicate that the semi-circular design has the most consistent airflow around its body, and the maximum pressure on the body is significantly lower in the semi-circular design than in the other designs.

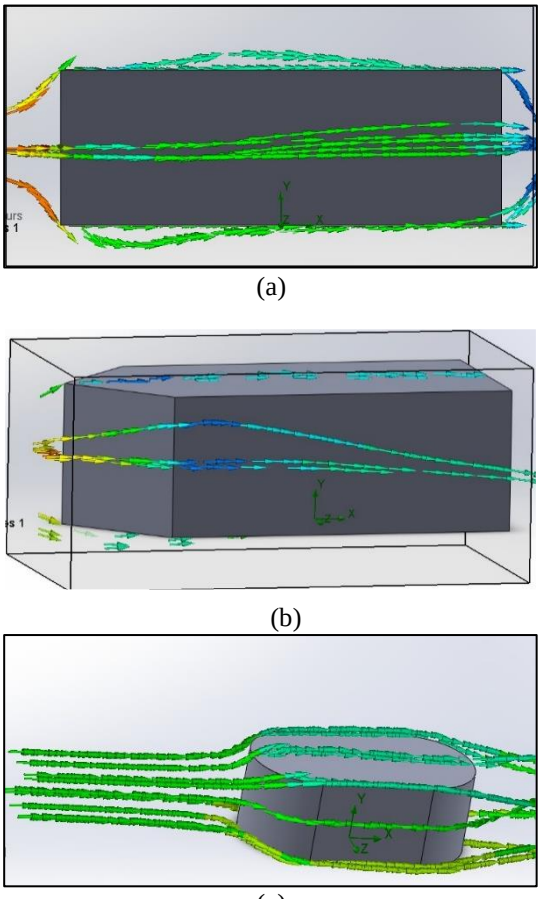

(a)

(b)

(c)

Fig. 3 Airflow simulation around the body of proposed models: (a) rectangular; (b) triangular; (c) semi-circular shape

B. General Design Parameter

The design Parameters discussed in Table 2 have been considered to establish the general requirements for the model. Motor selection, mechanical analysis, and CFD simulations are conducted according to the following requirements.

Table 2. Design parameters

Design Parameters	Value
Carrying payload	500 g
Maximum speed	2 m/s
Remote control range	10 m
0 to 2 m/s time	10 s
Skirt lifetime	2 h
Operational time	>15 min
Weight	4.5 kg
Dimensions	50x25x17.5 cm

C. Mechanical System

A small-scale, remotely controlled hovercraft proposed is depicted in Fig. 4 and detailed in Fig. 5, Fig. 6, and Table 3.

The majority of the proposed model components will be produced via 3D printing due to its cost-effectiveness and convenience. This model consists of two BLDC motors combined with propeller fans. One motor provides the required force to lift the hovercraft up, while the other motor (propulsion motor) provides the required force to move the hovercraft in the forward direction.

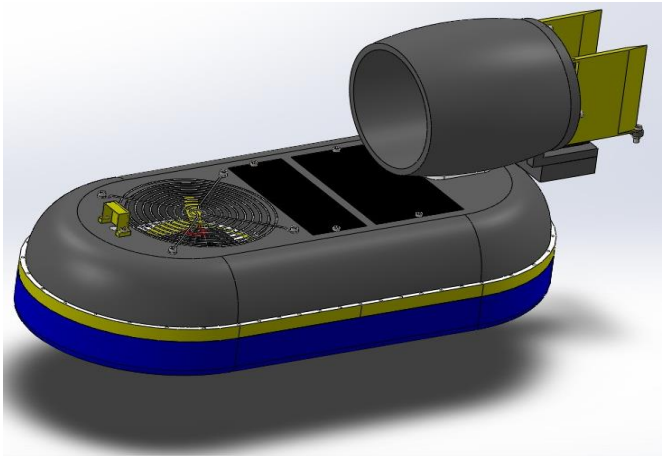

Fig. 4 3D Model of the proposed model

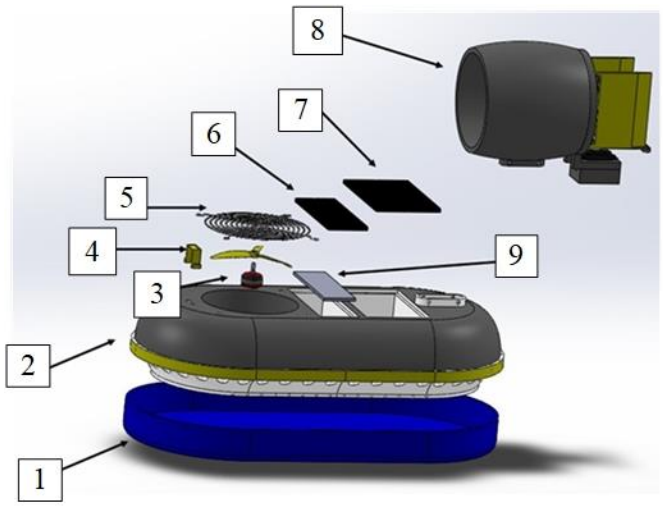

Fig. 5 Exploded view of the proposed model

A rudder system attached to the propulsion motor's assembly is designed to enable the hovercraft to move in different directions. The rudder system's angle is controlled by a servo motor.

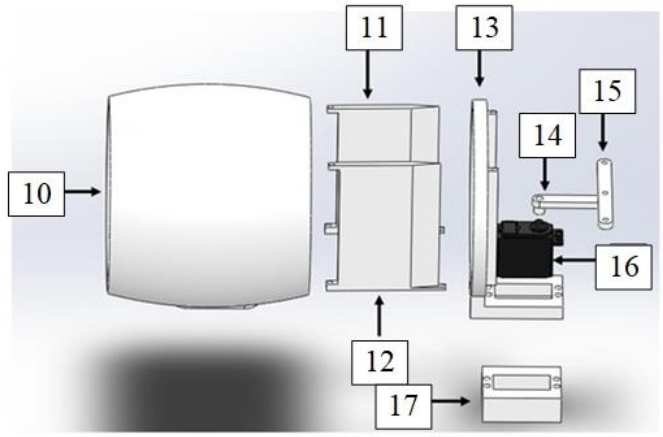

Fig. 6 Rudder system

Table 3. Parts of the hovercraft and used materials

	Part Name	Material
1	Skirt	Nylon
2	Hull	ABS
3	Motor and propeller	ABS for propeller
4	Camera protector	ABS + TPU
5	Lift fan protector	1060 Aluminum alloy
6	Payload cover	ABS
7	Electronic bay cover	ABS
8	Propulsion fan assembly	Mainly ABS
9	Load sensor cover	ABS
10	Thrust fan's shell	ABS
11	Rudder #1	ABS
12	Rudder #2	ABS
13	Thrust fan's bracket	ABS
14	Servo pin	ABS
15	Rudder pin	ABS
16	Servo motor	(---)
17	Servo Protector	ABS

D. Mechanical Analysis

In this section, utilizing Solidworks, various static analyses on the critical parts of the hovercraft have been conducted in order to verify the proposed model's safety and operational effectiveness.

- *Static Analysis of the Propeller*

Each propeller is subjected to the centrifugal force that is created by the motor and applied to the propeller. This force is applied at the center of the propeller which turns the propeller. Specification of the selected motor and propeller is summarized in Table 4 which has been considered in the Simulation.

Table 4. Specification of the motor and propeller

Specification	Value
Maximum RPM of the motor	20080 rpm
Maximum angular acceleration of the motor	0.024338 rpm^2
Propeller material	ABS
The ultimate strength of the ABS	27.6 – 55.2 MPa ≈ 41 MPa

The maximum stress on the propeller is 18.952 MPa which is below the ultimate strength of ABS material so we can use this propeller blade. Stress distribution on the propeller fan can be seen in Fig.7.

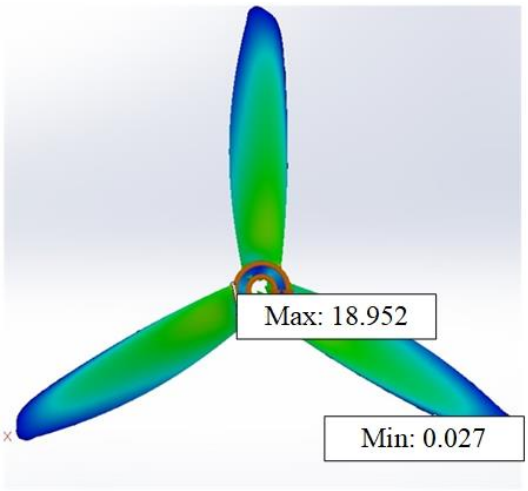

Fig. 7 Stress distribution on the propeller fan

- *Static Analysis Between Rudder and Rudder Bracket*

The harshest angle between the rudder and the back of the propulsion motor has been taken into consideration, notice that rudders don't need to have this harsh angle, but we assumed the harshest situation in this test. As expected the highest stress is in the connection points between the rudder and bracket. Maximum stress is around 8 MPa which is far below the ultimate strength of the ABS (41 MPa). Notice that no deformation or separation has happened so the result is satisfying.

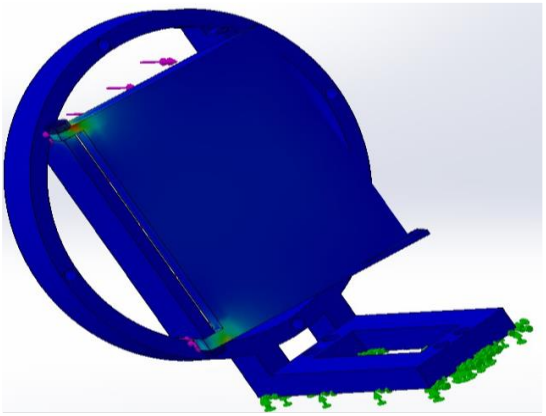

Fig. 8 Stress acting on the rudder and rudder bracket

- *Conjunction between Rudders and servo motor*

There is a torque applied by the servo motor to the rudder system, this force is used to rotate the rudders with the help of servo and rudder pins. The following Fig. 9 shows the centrifugal force applied by the servo motor to the servo pin. The selected servo motor has a maximum torque of 8 kg•cm and all materials employed in this proposed scaled hovercraft model are ABS.

The highest tensions are in conjunction areas, maximum tension is below the ultimate strength of ABS material, so this test satisfies our design.

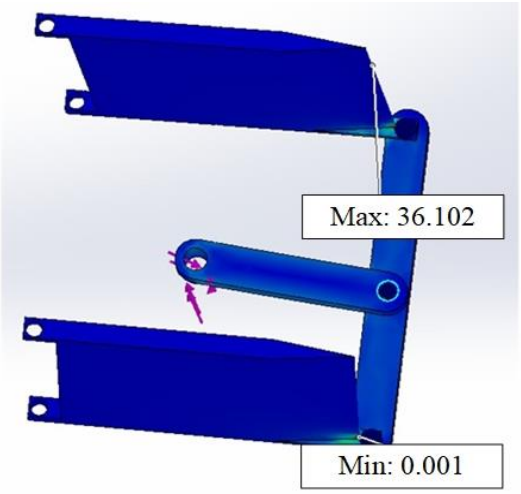

Fig. 9 Stress acting between the servo and rudder system

E. CFD Analysis

- *Drag Force Acting on the Body of Hovercraft*

To find the drag force acting on the hovercraft, an external flow simulation has been conducted in the Solidworks program. STP standards have been applied to the test, also the maximum velocity of the hovercraft is assumed to be 2 m/s. The flow has been considered as both laminar and turbulent, and the surrounding boundaries have been assumed to be adiabatic walls.

The flow of air trajectories is simulated as lines with arrows in Fig. 10, as it can be seen particles flow smoothly around the body and entrance of the lift fan. It is worth mentioning that there is small turbulence between the servo motor conjunction and the hovercraft's body, although the effect of this torbulance is neglecable, further studies can be done to reduce this effect. Results of our analysis show that the average drag force acting on the hovercraft is 0.105 N and the maximum force is 0.107 N.

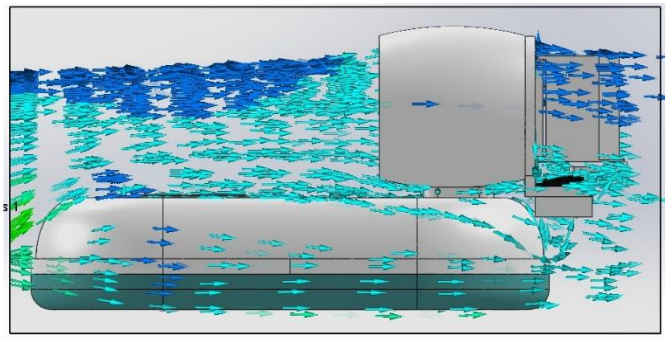

Fig. 10 Drag force analysis

- *Internal Flow Analysis*

An internal flow simulation is conducted to determine whether the chosen motor has enough power to lift the hovercraft up, also air flow inside the plenum chamber has been observed to ensure the stability of the airflow into the cushion. As can be seen in Fig. 11, arrows show the flow direction of the air which is directed to the plenum chamber by the lift fan's propeller. The simulation is conducted under STP standards and in the Solidworks program. Fig. 12 shows the average total pressure at the bottom of the air cushion. Be advised that is not gauge pressure and should be interpreted to gauge in order to check the results.

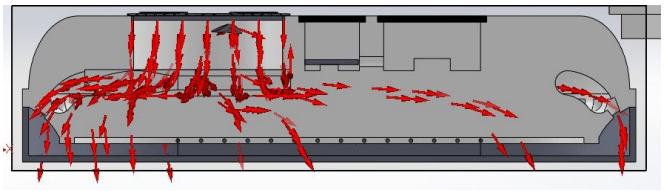

Fig 11. Internal airflow simulation

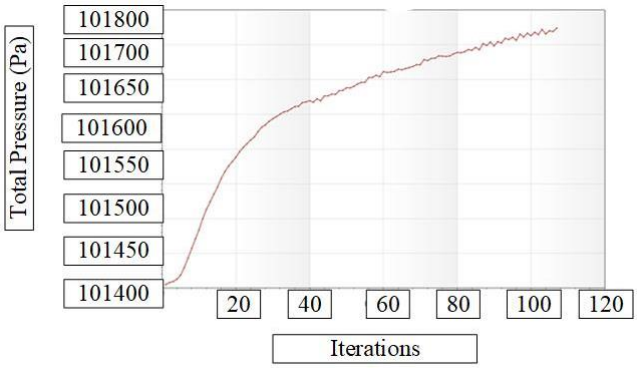

Fig.12 Average total pressure at the bottom of the cushion

IV. CONCLUSION

To use electric hovercrafts as an environmentally friendly mode of transportation, the initial design must emphasize energy efficiency. Flow analysis was utilized in this study to evaluate various geometries for the fundamental hovercraft structure. Based on the findings, a semi-circular structure was determined to be the most suitable option, and a design utilizing this configuration was proposed. In the future, our work schedule will include experimental testing and the proposal of a control method for the implementation of an adaptive lift fan. This paper also provides a comprehensive summary of the system topology and components for a small-scale model that will be used in future research.

REFERENCES

[1] J. R. Amyot, *Hovercraft Technology Economics and Applications*, 1st ed., Elsevier Science Publishers, Amsterdam, The Netherlands: 1989.

[2] A. Wang, H. Liu, S. Gao, C. Wu, "Analysis on Motion Stability and Safety of hovercraft in ice region," *The 6th International Conference on Transportation Information and Safety*., Oct. 2021.

[3] M. M. El-khatib, W. M. Hussein, "Stabilization and Design of a Hovercraft Intelligent Fuzzy Controller," *IJSRSET., vol .2, Dec. 2013*

[4] M. Riyadi, L. Rohmando, A. Triwiyatno, "Development of hovercraft prototype with stability control system using PID controller," *Int. Conf. on Information Tech., Computer, and Electrical Engineering.*, Oct.2016

[5] C. Wang, H. Zhang, M. Fu, Motion control of an amphibious hovercraft based on fuzzy weighting," *IEEE 14th International Conference on Communication Technology*., May. 2013

[6] L. Yun and A. Bliault, *Theory and Design of Air Cushion Craft*, 1st ed, London, UK: 2000,

[7] B. Gunston, *Hydrofoils and Hovercraft: New Vehicles for Sea and Land*, 1st ed, London, UK: Albus Book, 1969

[8] A. Dhale, A. Ahuja, P. Chanchal, R. Gupta, M. Kushwaha, "Design and Development of Hovercraft," *IJSRSET., vol. 2,* 2395-1990, *2016.*

[9] J. Anderson, "*Fundamentals of Aerodynamics*", 6th ed., McGraw Hill, New York, USA: 2016.

[10] S.V. Patankar, "*Numerical Heat Transfer and Fluid Flow*", 1st ed., McGraw-Hill, New York, USA: 1980.

[11] N. Saeid, E. Yunus, O. Fei, "CFD simulation of air flow around a hovercraft," *BICET 2014.*, Nov.2014

[12] T. Anter, Y. Hossamel-din, S. Abdrabbo, “An autonomous hovercraft with minimum energy consumption,” *International Conference on Research and Education in Mechatronics (REM),* Oct. 2107.

[13] S. M. Hein, H. C. Liaw, “Design and Development of a compact Hovercraft Vehicle,” - *2013 IEEE/ASME International Conference on Advanced Intelligent Mechatronics (AIM).*, vol. 2 9-12, Sep. 2013.

[14] M. El-Sharkawi, *Fundamentals of Electric Drives,* 2nd Ed., Cengage Learning, Boston, USA: 2018

[15] G. Eiffel, *The Resistance of The Air and Aviation*, 1st ed., Constable &Co Ltd, London, UK: 1914